

U.S. GOVERNMENT

OFFICE OF NAVAL RESEARCH
Contract N00014-86-K-0556
Technical Report No. 84

AD-A210 213

Redox-Induced Arene Hapticity Change in a
Mixed-Sandwich Rhodium(III)/(II)/(I) System:
An Illustrative Mechanistic Application of
Electron-Exchange Kinetics

by

R. M. Nielson and M. J. Weaver

Prepared for Publication

in

Organometallics

Purdue University
Department of Chemistry
West Lafayette, Indiana 47907

DTIC
ELECTE
JUL 18 1989
S D

July 1, 1989

Reproduction in whole, or in part, is permitted for any purpose of the United States Government.

* This document has been approved for public release and sale: its distribution is unlimited.

REPORT DOCUMENTATION PAGE

1a REPORT SECURITY CLASSIFICATION Unclassified		1b RESTRICTIVE MARKINGS	
2a SECURITY CLASSIFICATION AUTHORITY		3 DISTRIBUTION/AVAILABILITY OF REPORT Approved for public release and sale; its distribution is unlimited.	
2b DECLASSIFICATION/DOWNGRADING SCHEDULE			
4 PERFORMING ORGANIZATION REPORT NUMBER(S) Technical Report No. 84		5 MONITORING ORGANIZATION REPORT NUMBER(S)	
5a NAME OF PERFORMING ORGANIZATION Purdue University Department of Chemistry	6b OFFICE SYMBOL (if applicable)	7a NAME OF MONITORING ORGANIZATION Division of Sponsored Programs Purdue Research Foundation	
5c ADDRESS (City, State, and ZIP Code) Purdue University Department of Chemistry West Lafayette, Indiana 47907		7b ADDRESS (City, State, and ZIP Code) Purdue University West Lafayette, Indiana 47907	
8a NAME OF FUNDING/SPONSORING ORGANIZATION Office of Naval Research	8b OFFICE SYMBOL (if applicable)	9 PROCUREMENT INSTRUMENT IDENTIFICATION NUMBER Congract No. N00014-86-K-0556	
5c ADDRESS (City, State, and ZIP Code) 800 N. Quincy Street Arlington, VA 22217		10 SOURCE OF FUNDING NUMBERS	
		PROGRAM ELEMENT NO	PROJECT NO
		TASK NO	WORK UNIT ACCESSION NO
1 TITLE (Include Security Classification) Redox-Induced Arene Hapticity Change in a Mixed-Sandwich Rhodium(III)/(II)/(I) System: An Illustrative Mechanistic Application of Electron-Exchange Kinetics			
2 PERSONAL AUTHOR(S) R. M. Nielson and M. J. Weaver			
3a TYPE OF REPORT Technical	13b TIME COVERED FROM 10/1/87 TO 6/30/89	14 DATE OF REPORT (Year, Month, Day) July 1, 1989	15 PAGE COUNT
6 SUPPLEMENTARY NOTATION			
7 COSATI CODES		18 SUBJECT TERMS (Continue on reverse if necessary and identify by block number)	
FIELD	GROUP	redox-induced, arene hapticity, mixed-sandwich, phase-selective ac voltammetry, square-scheme mechanisms, concerted reaction pathways.	
9 ABSTRACT (Continue on reverse if necessary and identify by block number) Rate constants for homogeneous self exchange, k_{ex}^h , and electrochemical exchange, k_{ex}^e , have been measured for the first and second reduction steps of $(\eta^5-C_5Me_5)(\eta^6-C_6Me_6)M^{2+}$, where $M = Rh$ and Co , in order to assess the manner in which the $\eta^6 \rightleftharpoons \eta^4$ arene hapticity change observed upon formation of the Rh(I) two-electron reduction product is coupled with electron transfer. The analogous Co(III)/(II)/(I) mixed-sandwich system was chosen for comparison because, unlike Rh(III)/(II)/(I), the arene retains the η^6 configuration upon reduction. The k_{ex}^h values were evaluated in acetone, acetonitrile, and benzonitrile by utilizing the proton NMR line-broadening technique, and the k_{ex}^e values were obtained in these solvents and also nitrobenzene and propylene carbonate by using phase-selective ac voltammetry at an annealed gold electrode. The corresponding variations in k_{ex}^h and k_{ex}^e with the redox couple are shown to be uniformly consistent with the expectations of Marcus theory, indicating that the electrochemical as well as homogeneous-phase exchange kinetics refer to outer-sphere pathways, as desired. Both the Rh(III)/(II) and Rh(II)/(I) couples exhibit smaller rate constants in a (continued on back)			
20 DISTRIBUTION/AVAILABILITY OF ABSTRACT <input checked="" type="checkbox"/> UNCLASSIFIED/UNLIMITED <input checked="" type="checkbox"/> SAME AS RPT <input type="checkbox"/> DTIC USERS		21 ABSTRACT SECURITY CLASSIFICATION	
22a NAME OF RESPONSIBLE INDIVIDUAL		22b TELEPHONE (include Area Code)	22c OFFICE SYMBOL

Accession For	
NTIS GRA&I	<input checked="" type="checkbox"/>
DTIC TAB	<input type="checkbox"/>
Unannounced	<input type="checkbox"/>
Justification	
By	
Distribution/	
Availability Codes	
Avail and/or	
Dist	Special
A-1	

19. (cont.)

given solvent than the corresponding cobalt systems; while these differences are mild for the former couple, the rate constants for Rh(II)/(I) are substantially smaller (ca. 10^4 fold for k_{ex}^H) than for the other reactions. These rate differences indicate that the redox-induced hapticity change is coupled primarily to the second reduction step. Distinction is made between "square-scheme" mechanisms where the ligand conformational change is coupled to, but is microscopically separate from, the electron-transfer step, and "concerted" reaction pathways where the arene distortion forms part of the elementary electron-transfer barrier. Evidence that the mechanism for Rh(II)/(I) is at least partly concerted in nature is obtained from an analysis of the solvent dependence of k_{ex}^e , based on the anticipated influence of the ligand distortion in the electron-transfer barrier-crossing frequency. The stabilization afforded to Rh(I) by the $\eta^6 \rightarrow \eta^4$ conformational change is ascertained to be at least 6 kcal mol^{-1} .

**Redox-Induced Arene Hapticity Change in a Mixed-Sandwich
Rhodium(III)/(II)/(I) System: An Illustrative Mechanistic
Application of Electron-Exchange Kinetics**

Roger M. Nielson and Michael J. Weaver*

Department of Chemistry
Purdue University
West Lafayette, IN 47907

Organometallics
in press, March 1989

ABSTRACT

Rate constants for homogeneous self exchange, k_{ex}^h , and electrochemical exchange, k_{ex}^e , have been measured for the first and second reduction steps of $(\eta^5-C_5Me_5)(\eta^6-C_6Me_6)M^{2+}$, where $M = Rh$ and Co , in order to assess the manner in which the $\eta^6 = \eta^4$ arene hapticity change observed upon formation of the $Rh(I)$ two-electron reduction product is coupled with electron transfer. The analogous $Co(III)/(II)/(I)$ mixed-sandwich system was chosen for comparison because, unlike $Rh(III)/(II)/(I)$, the arene retains the η^6 configuration upon reduction. The k_{ex}^h values were evaluated in acetone, acetonitrile, and benzonitrile by utilizing the proton NMR line-broadening technique, and the k_{ex}^e values were obtained in these solvents and also nitrobenzene and propylene carbonate by using phase-selective ac voltammetry at an annealed gold electrode. The corresponding variations in k_{ex}^h and k_{ex}^e with the redox couple are shown to be uniformly consistent with the expectations of Marcus theory, indicating that the electrochemical as well as homogeneous-phase exchange kinetics refer to outer-sphere pathways, as desired. Both the $Rh(III)/(II)$ and $Rh(II)/(I)$ couples exhibit smaller rate constants in a given solvent than the corresponding cobalt systems; while these differences are mild for the former couple, the rate constants for $Rh(II)/(I)$ are substantially smaller (ca 10^4 fold for k_{ex}^h) than for the other reactions. These rate differences indicate that the redox-induced hapticity change is coupled primarily to the second reduction step. Distinction is made between "square-scheme" mechanisms where the ligand conformational change is coupled to, but is microscopically separate from, the electron-transfer step, and "concerted" reaction pathways where the arene distortion forms part of the elementary electron-transfer barrier. Evidence that the mechanism for $Rh(II)/(I)$ is at least partly concerted in nature is obtained from an analysis of the solvent dependence of k_{ex}^e , based on the anticipated influence of the ligand distortion in the electron-transfer barrier-crossing frequency. The stabilization afforded to $Rh(I)$ by the $\eta^6 \rightarrow \eta^4$ conformational change is ascertained to be at least 6 kcal mol⁻¹.

The factors giving rise to, and the attendant energetics of, changes in hapticity of metal arenes is a topic of substantial interest, especially given the likely relevance of such ring slippage to ligand substitution chemistry and the catalysis of arene hydrogenation.^{1,2} The observed arene ring slippage from hexapto (η^6) to tetrahapto (η^4) bonding can generally be understood in terms of the consequent attainment of the 18-electron configuration by the metal.^{1b} Not surprisingly, therefore, there are several documented examples of such η^6 to η^4 hapticity changes triggered by two-electron reduction of appropriate metal arenes.³⁻⁵ Besides the virtues of redox-induced reactions for preparative purposes, the elucidation of the mechanisms and energetics of the ligand structural transformations is of obvious fundamental importance.

One system of particular interest from this standpoint is provided by the reduction of η^5 -pentamethylcyclopentadienyl-(η^6 -hexamethylbenzene)-rhodium(III)[(η^5 -C₅Me₅)(η^6 -C₆Me₆)Rh²⁺, where Me = methyl].^{4,5} Two-electron reduction of this complex yields the tetrahapto Rh(I) complex (η^5 -C₅Me₅)(η^4 -C₆Me₆)Rh, similarly to several related ruthenium and iridium complexes (see Fig. 1).³⁻⁵ However, an unusual feature of the rhodium(III) complex is that it undergoes reduction via two electrochemically resolvable one-electron steps.^{4,5} This situation prompts the intriguing question of how the hapticity change, itself involving effectively a two-electron subtraction from the metal center, is coupled to these single-electron redox steps.

Several possibilities can be considered. Besides the general distinction between arene conformation changes that are triggered by the first or second (or both) reduction steps, the nature of this coupling is

expected to be different depending on whether or not such arene structural alterations occur separately from the elementary electron-transfer barrier itself. That is, it is possible that the ligand conformational change can constitute a microscopically separate step that, although driven by electron transfer, forms a distinct barrier on the potential energy-reaction coordinate profile. This conformational barrier may be situated either prior to or following the energy-transfer barrier. At least in the electrochemical literature, such mechanisms have become known as "square schemes", commonly designated by the notation "CE" or "EC" depending if the "chemical" (in this case, conformational) step occurs prior to or following the "electrochemical" (generally electron-transfer) step, respectively.⁶ However, the identification of CE and EC mechanisms (as well as more complex coupled schemes) is straightforward only for relatively long-lived intermediates, that are thereby susceptible to analytical detection.

As an alternative to such square-scheme mechanisms, the conformational change can be envisaged to occur at least partly *in concert* with the electron-transfer step. In this case, the reactant structural changes can form a "bond distortional" component of the electron-transfer barrier itself. That is, the alterations in reactant bond lengths and bond angles ("bond distortions") required to bring about the overall conformational change may form a component of the energy-reaction coordinate parabolas, also associated at least in part with nonequilibrium solvent polarization, at the intersection of which electron transfer can occur.⁷ This latter "concerted" (or "concurrent"^{6b}) pathway has been considered extensively for reactant distortional ("inner-shell") barriers associated with redox-induced alterations of metal-ligand bond distances, primarily for simple

inorganic reactions. For such systems, there is good evidence that the conventional, oft-termed⁶ "Marcus-Hush", model of concerted inner- and outer-shell (i.e. solvent) reorganization provides an appropriate description of the electron-transfer barrier.⁸

Indeed, it is not always recognized that the square-scheme description is necessarily inappropriate for such inner-shell distortions involving bound harmonic oscillators. This is because incurring the entire bond-distance alteration required to transform the reactant into product either before or after electron transfer will normally involve prohibitively large energies compared with pathways involving only partial bond distortion in the transition state for electron transfer.⁹ For ligand conformational changes on the other hand, such as the arene hapticity transformation considered here, one can envisage the entire structural transformation occurring either before or after electron transfer. This is because both conformational states may exhibit local free-energy minima (i.e. constitute microscopically stable species) even within the same formal redox state.⁶ Given that the less stable conformer in this scheme can be envisioned to suffer considerable "strain" associated with its nonoptimal electronic state, however, further reactant changes may nevertheless be required to occur concertedly with the electron-transfer step.

In either case, such ligand conformational changes are expected to exert a substantial influence upon the rate constants for the overall electron-transfer process. Experimental distinction between "square scheme" and "concerted" mechanisms will not be so straightforward when the structural changes are rapid and reversible, since only the rate constants and not the rate law will be affected. This situation applies to the

hapticity change considered here since both the Rh(III)/(II) and Rh(II)/(I) redox couples display chemically reversible behavior, at least on the cyclic voltammetric timescale.⁴ Nonetheless, a possible distinction between these mechanisms, which originally prompted the present study, is that processes involving substantial inner-shell structural distortions during the electron-transfer step should involve distinctly different dynamics to those where the structural change occurs separately. Thus for the latter mechanism, the frequency of surmounting the (presumably rate-determining) electron-transfer barrier will, at least for adiabatic processes,¹⁰ be dominated by solvent rather than the inner-shell motion that should influence the barrier-crossing dynamics in the former case.¹¹ As a consequence, the solvent dependence of the rate constants is anticipated to be distinctly different in these two cases.¹² The examination of rate-solvent dependencies could therefore constitute a viable, albeit so far unexplored, means of mechanism diagnosis.

The objective of the investigation reported here is to utilize solvent-dependent electron-transfer kinetic data obtained for the first and second reduction steps of $(\eta^5\text{-C}_5\text{Me}_5)(\eta^6\text{-C}_6\text{Me}_6)\text{Rh}^{2+}$, i.e. for the Rh(III)/(II) and Rh(II)/(I) redox couples, so to provide information on the mechanism as well as energetics of the η^6 to η^4 arene hapticity change engendered by reduction. Specifically, rate constants for homogeneous self exchange, k_{ex}^h , and electrochemical exchange, k_{ex}^e , were evaluated by using proton NMR line broadening, and ac and cyclic voltammetric measurements, respectively, for both the Rh(III)/(II) and Rh(II)/(I) steps in several solvents. These data are compared and contrasted with corresponding results obtained for the Co(III)/(II) and Co(II)/(I) couples formed from

the analogous cobalt complex $(\eta^5\text{-C}_5\text{Me}_5)(\eta^6\text{-C}_6\text{Me}_6)\text{Co}^{2+}$. Unlike its second-row rhodium analog, this cobalt complex remains in the same hapticity state even when fully reduced to Co(I) (*vide infra*).¹³

Taken together, the results indicate that the hapticity change in the rhodium system is coupled primarily with the second reduction step (cf ref. 4). They also suggest that the conformational and electron-transfer processes associated with this step may be partly concerted in nature. The solvent-dependent analysis presented here may have more general application for redox mechanistic purposes.

EXPERIMENTAL

Materials

Pentamethylcyclopentadienyl-(hexamethylbenzene)rhodium(III) bis(hexafluorophosphate) $[(\text{C}_5\text{Me}_5)(\text{C}_6\text{Me}_6)\text{Rh}\cdot(\text{PF}_6)_2]$ was synthesized in high yield from $(\text{C}_5\text{Me}_5\text{RhCl}_2)_2$, prepared as in ref. 14, and hexamethylbenzene (Aldrich) in refluxing trifluoroacetic acid as described in ref. 15. The analogous cobalt salt, $(\text{C}_5\text{Me}_5)(\text{C}_6\text{Me}_6)\text{Co}\cdot(\text{PF}_6)_2$, was synthesized from $(\text{C}_5\text{Me}_5\text{CoCl}_2)_2$, prepared as in ref. 16., and AlCl_3 /hexamethylbenzene in pentane at room temperature using a procedure similar to that described in ref. 17. The corresponding cobalt monocation, $(\text{C}_5\text{Me}_5)(\text{C}_6\text{Me}_6)\text{Co}\cdot\text{PF}_6$, was prepared by reducing the dication in methylene chloride with cobaltocene. The latter was isolated by the addition of toluene, and the product crystallized by evaporating the solvent under vacuum and cooling.

Tetraethylammonium tetrafluoroborate (TEAB, Aldrich) and potassium hexafluorophosphate (Aldrich), employed as supporting electrolytes, were each recrystallized twice from hot ethanol and water, respectively.

Tetrabutylammonium hexafluorophosphate (TBAH) was prepared by adding NH_4PF_6 to aqueous tetrabutylammonium bromide and twice recrystallizing from hot ethanol. The deuterated solvents acetonitrile, acetone, and methylene chloride (Aldrich), used in the NMR kinetic measurements, were distilled under argon from P_2O_5 , or CaSO_4 in the case of acetone. Protiated acetonitrile, acetone, propylene carbonate (Burdick and Jackson), nitrobenzene, benzonitrile (Fluka), and nitromethane (Mallinckrodt) were purified under argon using standard procedures.¹⁸

Kinetic Measurements

The rate constants for homogeneous self exchange, k_{ex}^{h} , were evaluated from proton NMR data collected on Nicolet NT200 and NT470 Fourier transform instruments operated at 200 and 469.5 MHz, respectively, chiefly as described previously.¹¹ All solution samples, containing appropriate mixtures of the diamagnetic and paramagnetic forms of the redox couple, were prepared within a N_2 -filled dry box using capped 5 mm glass tubes. Due to the relative instability of the Rh(II) complex,⁵ solutions were prepared by in-situ reduction of the Rh(III) species using either cobaltocene or the Rh(I) complex. Samples containing Rh(II) were frozen immediately in liquid N_2 after preparation, and removed just prior to NMR examination. Reactant concentrations were typically 20-30 mM in diamagnetic complex [Co(III), Rh(III), Rh(I)] and 1-15 mM in the corresponding paramagnetic complex [Co(II), Rh(II)]; the solution also contained 0.1 M KPF_6 or TEAB. Pertinent details of the NMR data analysis are described in the Results section.

The majority of rate constants for electrochemical exchange, k_{ox}° , were determined by using phase-selective ac voltammetry, chiefly as described in ref. 19. This utilized a PAR 173/179 potentiostat, a PAR 175 potential programmer, a PAR 5204 lock-in amplifier, a Hewlett-Packard 3314A function generator, and a Fluka 1900A frequency counter. The in-phase and quadrature currents, from which the phase angle ϕ was obtained, were displayed simultaneously using a pair of X-Y recorders. The k_{ox}° values were extracted from the slopes of $\cot \phi - \omega^2$ plots, with the frequency ω being varied over the range 50 to 1000 Hz. The electrochemical transfer coefficients, extracted as noted in ref. 19, were generally found to approximate 0.5 (± 0.1). In each case, a 1-2 mM solution of the Rh(III) or Co(III) complex was used.

The k_{ox}° values for the Rh(II)/(I) couple were typically too small to yield sufficient ac responses. These rate constants were instead obtained by using cathodic-anodic cyclic voltammetry at sweep rates from 0.1 to 2 V s^{-1} , employing the procedure of Nicholson.²⁰ The voltammograms were displayed on an Hewlett Packard 7045B XY recorder, or a Nicolet Explorer I storage oscilloscope. The diffusion coefficients required for both ac and cyclic voltammetric data analyses were obtained from dc polarographic limiting currents, using a dropping mercury electrode.

Both gold and mercury were employed as working electrodes; however, most measurements utilized the former surface (vide infra). The gold surface was a bead of ca 1 mm diameter. It was pretreated immediately prior to use by heating to just below the melting point in a propane-oxygen flame. This pretreatment was found to yield unusually reproducible and stable electrochemical kinetic behavior. Positive-feedback IR compensation

was employed in all rate measurements in order to eliminate, or at least minimize, the influence of solution resistance.^{19,21} All electrode potentials were measured and are quoted versus an aqueous saturated calomel electrode (SCE).

RESULTS

As already noted, the overall strategy employed here entails evaluating k_{ox}^h and k_{ox}° values for the Rh(III)/(II) and Rh(II)/(I) couples in comparison with corresponding data for the analogous Co(III)/(II) and Co(II)/(I) steps. The electron-exchange kinetics were evaluated in both homogeneous-phase and electrochemical environments for several reasons. While the homogeneous self-exchange kinetics correspond to clearcut outer-sphere mechanisms as desired, the evaluation of k_{ox}^h by NMR line broadening requires both redox forms to be stable on the timescale (\geq several minutes) required for these measurements. The limited stability of the Rh(II) complex⁵ limits severely the range of solvents and physical conditions for which k_{ox}^h for the Rh(III)/(II) and Rh(II)/(I) couples can be evaluated (vide infra). In addition, the Co(I) as well as the Co(II) complex is paramagnetic,¹³ thereby thwarting NMR kinetic measurements for the Co(II)/(I) couple.

The reactant stability requirements are less stringent for the electrochemical exchange measurements, since the electrogenerated species need only be stable over the diffusion-layer lifetime ($ca \leq 10^{-2}$ s). As a consequence, k_{ox}° values could be obtained for all four redox couples of interest here. An apparent limitation of the electrochemical kinetic measurements for the present purpose is that the k_{ox}° values are (or are

commonly perceived to be) influenced significantly by adsorption and other interfacial effects.^{4,6} However, well-known relationships between corresponding k_{ox}^o and k_{ox}^h values, originally derived by Marcus,²² should apply when both the electrochemical and homogeneous-phase exchange processes refer to outer-sphere pathways and the work terms are relatively small or constant. Both k_{ox}^h and k_{ox}^o values for a given redox couple were acquired whenever feasible in this work, and examined in this manner so to provide a check on the possible presence of mechanistic complications.

Table I summarizes the rate constants for homogeneous-phase self exchange obtained here, determined by using proton NMR line broadening. The NMR spectra for the Rh(III)/Rh(II) mixtures contained peaks identified with the C_5Me_5 and C_6Me_6 ring protons on Rh(III), having the same chemical shifts as for the pure diamagnetic Rh(III) complex. The line width (at half height) for the mixture, ω_{DP} , increased both with increasing temperature and linearly with increasing Rh(II) concentration. This behavior indicates that the electron exchange process lies within in the NMR "slow exchange limit", whereupon k_{ox}^h can be obtained from²³

$$k_{ox}^h = \pi C_p^{-1} (\omega_{DP} - \omega_D) \quad (1)$$

where C_p is the concentration of the paramagnetic species and ω_D is the line width of the pure diamagnetic species.

Equation (1) was used to obtain k_{ox}^h for Rh(III)/(II) and Rh(II)/(I) in acetone- d_6 by measuring ω_{DP} for a series of samples containing varying C_p and a constant diamagnetic species concentration, and extracting k_{ox}^h from the $(\omega_{DP} - \omega_D) - C_p$ slope. However, the stability of the Rh(II) complex in acetonitrile- d_3 is insufficient at room temperature to enable this

procedure to be employed. Instead, k_{ox}^h values over the temperature range -35 to 0°C were determined using four separate (i.e. fresh) samples, enabling k_{ox}^h at 25°C to be obtained by extrapolation using the Arrhenius equation. These measurements utilized a field strength of 470 MHz in order to yield a satisfactory resolution of the various peaks. Attempts to evaluate k_{ox}^h for Rh(II)/(I) in acetonitrile and benzonitrile were thwarted by insufficient solubility of the Rh(I) complex coupled with Rh(II) decomposition.

Mixtures of the Co(III) and Co(II) complexes yielded proton NMR spectra having a single pair of peaks due to the C_5Me_5 and C_6Me_6 ligands, having chemical shifts that are intermediate between those measured for the pure Co(III) and Co(II) solutions. This indicates that the electron exchange process falls within the NMR "fast exchange" region, enabling k_{ox}^h to be obtained from the linewidth and chemical shift data by using the procedure outlined in ref. 11. Values of k_{ox}^h were determined in this manner for the Co(III)/(II) couple in acetone- d_6 , acetonitrile- d_3 , and benzonitrile. The values reported in Table I are the average of at least two determinations; they were reproducible at least to within $\pm 20\%$.

Where both the reactants are charged, as for Rh(III)/(II) and Co(III)/(II) where the charge numbers on the oxidized and reduced species are $Z_1 = 2$ and $Z_2 = 1$, respectively, it is desirable to correct k_{ox}^h for electrostatic work terms. A commonly used expression is²⁴

$$k_{ox}^h(\text{cor}) = k_{ox}^h \exp(w_r/RT) \quad (2)$$

$$w_r = Z_1 Z_2 N [\epsilon_s r (1 + Br\mu^h)]^{-1} \quad (2a)$$

where ϵ_s is the static solvent dielectric constant, N is the Avogadro

number, B is the Debye-Huckel parameter, r is the reactant internuclear distance, and μ is the ionic strength. The $k_{ox}^h(\text{cor})$ values given in Table I were obtained from Eq. (2) by assuming that $r = 7.6 \text{ \AA}$ (i.e. twice the reactant radius, ca 3.8 \AA^{11}).

A summary of the corresponding electrochemical rate constants, k_{ox} , evaluated for the Rh(III)/(II), Rh(II)/(I), Co(III)/(II), and Co(II)/(I) couples is provided in Table II. The five solvents chosen, acetonitrile, acetone, benzonitrile, nitrobenzene, and propylene carbonate, were selected not only so to yield corresponding electrochemical rate information to that in Table I but also to provide a range of solvent dynamical behavior (vide infra). All the data in Table II were obtained at gold and for solutions containing 0.1 M tetrabutylammonium hexafluorophosphate (TBAH). Substitution with 0.1 M tetraethylammonium hexafluorophosphate yielded essentially identical results within the reproducibility of the k_{ox}° values, typically $\pm 20\%$. Increasing the electrolyte concentration to 0.5 M TBAH yielded increases in k_{ox}° of typically 1.5 to 2 fold for the Rh(III)/(II) and Co(III)/(II) couples, with smaller (≤ 1.5 fold) increases for the corresponding M(II)/(I) couples. In view of the uncertainties in the validity of double-layer (i.e. work term) corrections for these systems, they were not applied. This is of little consequence for the present purposes since we are interested primarily in the relative rate constants as a function of solvent and reactant composition (vide infra); the magnitude of the double-layer corrections is unlikely to vary greatly under these conditions.

The Co(III)/(II) and Co(II)/(I) couples also yielded closely similar k_{ox}° values on mercury to those on gold, generally being within ca 50% of

each other. However, both the Rh(II)/I) as well as the Rh(III)/(II) couple yielded k_{ox}° values on mercury in all solvents studied here that are uniformly above the upper measurement limit, ca $2-7 \text{ cm s}^{-1}$ (This limit depends somewhat on the solvent)^{19,21}. Although the ac voltammograms on mercury showed no obvious signs of distortions (i.e. additional peaks, etc.), this surprising behavior seems most likely to be due to reactant adsorption, possibly arising from specific rhodium-mercury interactions.

DISCUSSION

Consistency of Homogeneous and Electrochemical Kinetic Data

At the outset, it is desirable to compare the homogeneous-phase and electrochemical kinetic data in order to ascertain if they are self consistent within the expectations of outer-sphere rate formalisms. If this is the case, according to the usual dielectric continuum model²² we expect k_{ox}° and k_{ox}^h to be related by^{25,26}

$$2 \log(k_{ox}^{\circ}/A_{\circ}) - \log(k_{ox}^h/A_h) - C/2.3RT \quad (3)$$

where

$$C = (e^2/4)(r_h^{-1} - r_{\circ}^{-1})(\epsilon_{op}^{-1} - \epsilon_s^{-1}) \quad (3a)$$

Here r_h and r_{\circ} are the internuclear distance between the homogeneous reacting pair and twice the reactant-electrode (i.e. the charge-metal image) distance, respectively, e is the electronic charge, ϵ_{op} and ϵ_s are the optical and static dielectric constants, and A_{\circ} and A_h are the appropriate electrochemical and homogeneous-phase preexponential factors.

Testing the degree of conformity of the experimental data to Eq. (3)

is complicated by several factors. Specifically, the estimation of A_o and A_h is dependent on the statistical models employed and the degree of reaction adiabaticity, and the importance of the C term depends on the details of the homogeneous and electrochemical reaction geometries.^{7b,25} Nevertheless, by utilizing reasonable estimates of these parameters, the corresponding values of k_{ox}^h and k_{ox}^o for a given redox couple and solvent in Tables I and II can be shown to be in reasonable concordance.²⁸ For the present purpose, however, we are concerned primarily with the corresponding variations in k_{ox}^o and k_{ox}^h brought about by structural alterations in the redox couple. Under these conditions, C as well as A_o and A_h should remain roughly constant so that from Eq. (3) we predict that simply

$$2 \Delta \log k_{ox}^o = \Delta \log k_{ox}^h \quad (4)$$

This relationship arises because a pair of structurally similar reactants need to be activated in the homogeneous reaction rather than a single reactant as in the electrochemical case.

Inspection of the corresponding k_{ox}^h and k_{ox}^o values in Tables I and II reveals that the rate differences observed between the Rh(III)/(II), Rh(II)/(I), and Co(III)/(II) couples in the electrochemical and homogeneous-phase environments are reasonably consistent with Eq. (4). In particular, the ca 500 fold smaller k_{ox}^h value for the Rh(II)/(I) compared to the Rh(III)/(II) couple in acetone (Table I) is matched well by the square of the corresponding k_{ox}^o ratio, ca 25 (Table II). The 3-5 fold smaller k_{ox}^o values obtained in acetonitrile and acetone for the Rh(III)/(II) versus the Co(III)/(II) couple is also roughly consistent with the corresponding k_{ox}^h ratio in the latter solvent. Even though these

comparisons are necessarily limited, they provide ample evidence that the more extensive electrochemical, as well as the homogeneous-phase, rate data indeed refer to simple outer-sphere pathways.

Mechanism of Redox-Induced Hapticity Change

On this basis, then, we feel justified in interpreting the kinetic data in Table I and II in a unified fashion with the objective of examining the underlying structural changes coupled to the electron-transfer steps. Geiger and coworkers have presented evidence, primarily from electrochemical thermodynamic measurements, that suggest strongly that the arene hapticity change for the $(C_5Me_5)(C_6Me_6)Rh^{2+/+/0}$ [Rh(III)/(II)/(I)] system is coupled to the second step, i.e. Rh(II)/(I).^{4,5} Retention of the η^6 -arene configuration for the Rh(II) complex is also indicated from temperature-dependent NMR measurements.²⁹ The markedly smaller k_{ox}^h and k_{ox}^o seen for the Rh(II)/(I) step in comparison with the corresponding values for the Rh(III)/(II) couple in Tables I and II lend strong support to this assertion.

Further insight into the mechanisms as well as energetics of the structural changes involved can be obtained from a more detailed perusal of the kinetic data. First, it is interesting to note that the rate constants for the Rh(III)/(II) step, although substantially greater than for Rh(II)/(I), are still significantly (typically 3-5 fold) smaller than for the corresponding Co(III)/(II) couple (Tables I, II). This result is suggestive that the metal-ligand geometry in $(\eta^5-C_5Me_5)(\eta^6-C_6Me_6)Rh^{2+}$ undergoes mild distortion upon one-electron reduction to Rh(II).

Before accepting this conclusion, however, it is instructive to

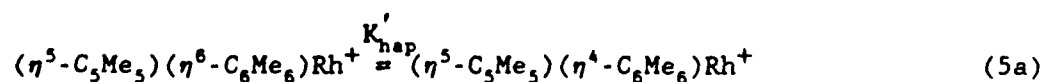
compare briefly the exchange kinetics for these systems with those for related metallocene couples, recently examined in our laboratory.^{11,19,30} Even after correction for electrostatic work, the rate constants for $(C_5Me_5)(C_6Me_6)Co^{2+/+}$ self exchange in acetonitrile, acetone, and benzonitrile [$k_{ex}^h(\text{cor})$, Table I] are somewhat (ca 10 fold) smaller than the corresponding k_{ex}^h values obtained for the structurally similar and isoelectronic $(C_5Me_5)_2Co^{+/0}$ couple.¹¹ The latter system exhibits facile electron-transfer kinetics; a range of smaller k_{ex}^h values have been observed for other cobaltocenium-cobaltocene and ferrocenium-ferrocene couples, such that the rate constants for $Cp_2Fe^{+/0}$ are around 50 fold smaller than for $(Cp-Me_5)_2Co^{+/0}$ in these solvents.^{11,30,31} These rate differences have been diagnosed as arising primarily from variations in the degree of donor-acceptor orbital overlap, i.e. in the efficiency of electron tunneling.^{30b,31} This conclusion makes use of the known small structural distortions together with the extensive molecular orbital studies which have been undertaken for these simple metallocenes.³¹

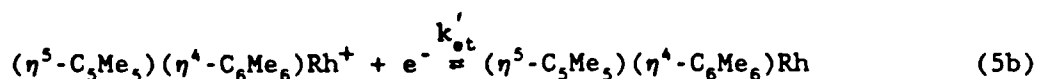
In the absence of such detailed structural information for the $(C_5Me_5)(C_6Me_6)Co^{2+/+}$ as well as the $(C_5Me_5)(C_6Me_6)Rh^{2+/+}$ redox couples, the possibility should be considered that the observed slower kinetics for the latter may be due to orbital overlap factors rather than the presence of inner-shell structural distortion. However, the former appears unlikely given that the Rh(III)/(II) couple should be characterized by greater donor-acceptor electronic coupling than the analogous Co(III)/(II) system as a result of the enhanced spatial extension of the d-orbitals expected for the second- versus the first-row transition metal. This expectation is upheld by the markedly (2.5 fold) larger NMR contact shifts for both the

arene and cyclopentadienyl ligands for the Rh(III)/(II) versus the Co(III)/(II) couple, which are indicative of greater ring electron density in the reduced state for the former couple.³²

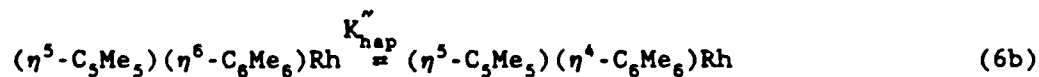
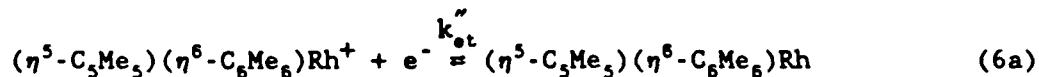
We are therefore confident in asserting that the smaller k_{ox}^h and k_{ox}^o values for Rh(III)/(II) versus Co(III)/(II) signal the presence of an additional structural distortion required for the former reaction. Nevertheless, the difference is energetically small, amounting to about 1 kcal mol⁻¹ for the self-exchange activation energy, ΔG_h^* , or only 0.5 kcal mol⁻¹ for the redox conversion of a single complex, as in the electrochemical exchange process. One can envisage this barrier as being associated with a small additional degree of metal-ring (and/or inter-ring) bond distortion associated with forming the 19e⁻ rhodium complex, given that both rings are especially electron-rich in the reduced state.

The very much slower exchange kinetics of the Rh(II)/(I) couple as compared both to Rh(III)/(II) and Co(II)/(I) are clearly indicative of the occurrence of major structural alterations associated with the first reaction. In discussing the mechanistic and energetic consequences of these findings, it is convenient to first consider a "square-scheme" mechanism. Although related treatments are available,^{6b,33} a pertinent discussion of the implications of such mechanisms on the overall electron-transfer kinetics has apparently not been provided previously, prompting the following. Two possibilities suggest themselves, involving the hapticity change occurring either just before, or following, the electron-transfer step, i.e. via "CE" or "EC" mechanisms:





or



As written, both these mechanisms refer to electrochemical rather than homogeneous exchange processes. The discussion here will be couched in terms of the former type since the mechanistic designation is simpler (or perhaps less confusing!) when only a single reacting species is involved. Nevertheless, given that homogeneous self exchange can be perceived as energetically equivalent to a pair of corresponding electrochemical reactions coupled "back-to-back",^{7b,34} yielding Eq. (4), their interrelation is straightforward.

Provided that electron transfer is indeed the rate-determining step and the coupled conformational change is sufficiently rapid to be in quasi-equilibrium, the overall rate constant k_{ex}° will be affected only by the equilibrium constant of the latter step [K_{hap} in Eqs. (5a) and (6a)]. Although perhaps not obvious from the form of Eqs. (5) and (6), the presence of such a rapid chemical step either before or after electron transfer will decrease k_{ex}° in the same fashion. This is because the thermodynamics of the electron-transfer step will be affected similarly in either case, given that the overall free-energy driving force is necessarily zero for an exchange process. The situation here is entirely analogous to the oft-considered influence of so-called work terms in electron-transfer kinetics, associated with forming the precursor and successor states from the separated reactants and products, respectively.

In this case, it is simple to show that the influence of K_{hap} upon k_{ox} for a CE mechanism [Eq. (5)] is given by³⁵

$$k_{ox} = (K'_{hap})^{1/2} k_{ox}^0 \quad (7)$$

where k_{ox}^0 is the rate constant that would be observed if the hapticity change involved a zero free-energy driving force (or, equivalently, in the absence of the hapticity change). Similarly, for the corresponding EC mechanism [Eq. (6)] we obtain³⁵

$$k_{ox} = (K''_{hap})^{-1/2} k_{ox}^0 \quad (8)$$

While Eqs. (7) and (8) necessarily refer to electrochemical rate data, the same analysis applies to homogeneous self-exchange kinetics simply by combining these relations with Eq. (4). It is clear that no obvious distinction can be made between the CE and EC mechanisms from the rate data alone in view of the equivalent forms of Eqs. (7) and (8). Therefore, for convenience here we will assume that the latter prevails, i.e. the hapticity change follows the second electron-transfer step, and will therefore consider K''_{hap} .

The application of Eqs. (7) and (8) to the experimental kinetics for Rh(II)/(I) requires estimates of k_{ox}^0 . For the electrochemical case, an approximate estimate can be obtained from the k_{ox}^0 value for the Co(II)/(I) couple in the same solvent. In acetone, for example, this procedure yields $K''_{hap} \sim 1.5 \times 10^4$. A similar estimate of K''_{hap} , ca 3.5×10^4 , is obtained using the k_{ox}^h value for Rh(II)/(I) in acetone, along with the corresponding $k_{ox}^h(\text{cor})$ value for Co(III)/(II). While smaller K''_{hap} values are obtained from the electrochemical data in most other solvents, this probably arises

in part from a breakdown of the assumption, embodied in Eqs. (7) and (8), that the preexponential factors for k_{ox} and k_{ox}^o are the same³⁵ (vide infra).

Irrespective of whether the hapticity change is perceived to occur before or after electron transfer, on the basis of this square-scheme analysis we predict that the free-energy stabilization afforded to the Rh(I) complex by the $\eta^6 \rightarrow \eta^4$ distortion, $-\Delta G_{hap}^o$, is about 5.5 to 6 kcal mol⁻¹ (since $-\Delta G_{hap}^o = RT \ln K_{hap}^{\sim}$). Even if the square-scheme mechanism is entirely valid, however, this estimate is only approximate (and possibly too large) given the assumptions involved in obtaining Eqs. (7) and (8). It is interesting to note that Bowyer and Geiger arrived at a somewhat larger estimate of $-\Delta G_{hap}^o$, about 9 kcal mol⁻¹, based on a consideration of formal potential data.⁴ The latter as well as the former ΔG_{hap}^o estimates are somewhat tentative. Nevertheless, if a pure square-scheme mechanism were indeed being followed, one would expect a better concordance between these ΔG_{hap}^o estimates since the analysis presumes that the influence of the conformational changes on the electron-transfer kinetics is entirely thermodynamic in origin. If, however, the actual reaction mechanism involves the hapticity change occurring at least partially in concert with electron transfer, this analysis will yield $-\Delta G_{hap}^o$ estimates that are indeed smaller than the actual value. This is because alternative concerted pathways will control the observed kinetics if they lead to larger k_{ox} values than those corresponding to pure square-scheme routes, necessarily yielding smaller K_{hap}^{\sim} and hence $-\Delta G_{hap}^o$ estimates.

Reaction Mechanism: Evidence from Solvent-Dependent Kinetics

Somewhat more direct evidence that the bond hapticity change occurs in a least partially concerted fashion with the electron-transfer step is obtained by examining the solvent dependence of the electrochemical rate constants. As already mentioned, if the entire inner-shell structural change occurs separately to the electron-transfer step, the adiabatic barrier-crossing frequency, ν_n , should be controlled by the dynamics of solvent reorganization and will therefore be sensitive to the solvent medium employed.^{11,19} On the other hand, if the inner-shell distortion forms a significant component of the elementary electron-transfer barrier (i.e. a "concerted" mechanism applies), then ν_n will be determined at least partly by the generally faster inner-shell dynamics such that its solvent dependence can be muted or even eliminated.^{11,12} Consequently, examining the solvent dependence of k_{ox}° for the Rh(III)/(II) and especially Rh(II)/(I) couples in comparison with corresponding data for the Co(III)/(II), Co(II)/(I), and other couples for which the inner-shell distortions are small can shed light on the reaction mechanisms for the former systems.

Table III contains ratios of k_{ox}° values measured in four solvents with respect to the corresponding value in acetonitrile, $k_{ox}^{\circ}/k_{ox}^{\circ}(\text{AN})$, for several redox couples, including the mixed-sandwich rhodium and cobalt systems of interest here. The four solvents chosen, benzonitrile, nitrobenzene, propylene carbonate, and acetone are known to exhibit widely varying solvent dynamical properties with respect to acetonitrile.^{11,19} In particular, the first two solvents exhibit much slower dynamics than acetonitrile or acetone, so that markedly different $k_{ox}^{\circ}/k_{ox}^{\circ}(\text{AN})$ ratios are

predicted depending on whether ν_n is controlled primarily by inner- or outer-shell (i.e. solvent) dynamics.^{11,19a} Thus we can express the rate ratios as

$$k_{ox}/k_{ox}(AN) = [\nu_n/\nu_n(AN)] \exp[(\Delta G_{AN}^* - \Delta G^*)/RT] \quad (9)$$

where $\nu_n(AN)$ and ΔG_{AN}^* are the nuclear frequency factor and activation free energy pertaining to the reaction in acetonitrile.

Inspection of Table III shows that indeed the $k_{ox}^*/k_{ox}^*(AN)$ ratios for the Rh(II)/(I) and Co(II)/(I) couples are markedly different in benzonitrile. While the rate ratios are determined in part by the solvent-dependent barriers [Eq. (9)],¹⁹ these should be sensitive only to the solvent rather than the redox couple, so that the differences in $k_{ox}/k_{ox}(AN)$ between Rh(II)/(I) and Co(II)/(I) can be ascribed chiefly to variations in $\nu_n/\nu_n(AN)$. The markedly (5 fold) larger $\nu_n/\nu_n(AN)$ ratio for the former couple in benzonitrile is indicative of the influence of inner-shell motion upon ν_n since this would have the effect of muting the effect of the ca 20 fold slower solvent dynamics of benzonitrile versus acetonitrile.¹⁹

Also included for comparison in Table III are $k_{ox}^*/k_{ox}^*(AN)$ ratios determined at gold for a pair of redox couples $Co(dmgs)_3(BF)_2^{+/0}$ and $Co(dmgs)_3(BC_4H_9)_2^{+/0}$ (dmg = deprotonated dimethylglyoxime)³⁶ that are known to involve substantial concerted inner-shell barriers³⁷ as well as $Cp_2Co^{+/0}$ (Cp = cyclopentadienyl) for which the bond-distortional barrier is small.¹⁹ Consistent with these arguments, the former couples yield comparable $k_{ox}^*/k_{ox}^*(AN)$ ratios in benzonitrile to those for Rh(II)/(I), whereas the behavior of $Cp_2Co^{+/0}$ is similar to Co(II)/(I) (Table III; see refs. 19 and

36 for detailed data analyses and discussion).

Interestingly, the Rh(III)/(II) couple also displays a relatively large $k_{ox}^{\circ}/k_{ox}^{\circ}(AN)$ ratio in benzonitrile, suggestive of a concerted bond distortional-electron transfer pathway. Given that the extent of inner-shell distortion associated with the Rh(III)/(II) step is necessarily small, however, this observation does highlight the possibility that the hapticity change and electron transfer for Rh(II)/(I) may occur in only a partly concerted fashion. In any case, the mechanistic conclusions based on these observations can only be regarded as being useful in a qualitative vein.

The $k_{ox}^{\circ}/k_{ox}^{\circ}(AN)$ ratios observed in other solvents (Table III) are also consistent with the above arguments. Comparable rate ratios are observed in nitrobenzene and benzonitrile, as expected in view of the similar dielectric and dynamical properties of these two solvents. Larger $k_{ox}^{\circ}/k_{ox}^{\circ}(AN)$ ratios for Rh(III)/(II) and especially Rh(II)/(I) relative to those for Co(III)/(II) and Co(II)/(I) are also observed in propylene carbonate. The small differences in $k_{ox}^{\circ}/k_{ox}^{\circ}(AN)$ between the various redox couples in acetone are expected in view of the similar dynamical properties of acetone and acetonitrile.^{11,19}

Concluding Remarks

While some aspects of the redox-induced $\eta^6 = \eta^4$ hapticity change in the mixed-sandwich Rh(III)/(I) system remain unclear, the present findings not only provide direct evidence for the coupling of this transformation to the Rh(II)/(I) step, but also demonstrate that the simple "square-scheme" mechanism provides a somewhat oversimplified description. The likelihood

that the conformational change occurs in an at least partly concerted manner with electron transfer, as deduced from the solvent-dependent kinetic analysis, is perhaps not surprising. Even the transient formation of the 20-electron Rh(I) product with complete retention of the η^6 -arene configuration would seem unlikely given the considerably (≥ 6 kcal mol⁻¹) greater stability of the corresponding η^4 state. The occurrence of at least some distortion away from ring planarity concomitant with cresting the Rh(II) = Rh(I) electron-transfer barrier provides one means by which the incipient Rh(I) state could be stabilized. The likely occurrence of some additional (albeit minor) ring distortion concertedly with the Rh(III) = Rh(II) step, as also suggested by the rate data, provides further evidence that the η^6 to η^4 transformation is energetically unlikely to occur entirely within a given rhodium redox state.

The limitations of employing electrochemical kinetic data to infer the presence of redox-induced molecular structural transformations in organometallic systems have been enumerated upon recently on more than one occasion (e.g. refs. 4,6,38). These concerns are undoubtedly valid in some cases, especially when reactant and/or product adsorption is suspected or when the rates approach the upper limit of the technique being employed. We do not, however, regard them as a justification for neglecting or abandoning such tactics. Mechanistic self-consistency checks can often be made from systematic kinetic measurements under different reaction conditions, especially in homogeneous-phase as well as electrochemical environments as in the present case. At least in favorable circumstances, there is good reason to regard such kinetic measurements as a valuable source of mechanistic information.

Acknowledgments

Conversations with Professor W. E. Geiger contributed significantly to the data interpretation. The NMR instruments used here are supported by National Institutes of Health and National Science Foundation Grants RR 01077 and BBS-8714253, respectively. This work is supported in part by the Office of Naval Research.

References and Notes

1. (a) Muetterties, E. L.; Bleeke, J. R., *Acc. Chem. Res.*, 1979, 12, 324; (b) Muetterties, E. L.; Bleeke, J. R.; Wucherer, E. J.; Albright, T. A., *Chem. Rev.*, 1982, 82, 499.
2. For example, (a) Landis, C. R.; Halpern, J., *Organometallics*, 1983, 2, 840; (b) Traylor, T. G.; Stewart, K. J.; Goldberg, M. J., *J. Am. Chem. Soc.*, 1984, 106, 4445.
3. (a) Kang, J. W.; Childs, R. F.; Maitlis, P. M., *J. Am. Chem. Soc.*, 1970, 92, 720; (b) Barbatì, A.; Calderazzo, F.; Poli, R.; Zanozzi, P. F., *J. Chem. Soc. Dalton Trans.*, 1986, 2569; (c) Finke, R. G.; Voegeli, R. H.; Laganis, E. D.; Boekelhelde, V., *Organometallics*, 1983, 2, 347.
4. Bowyer, W. J.; Geiger, W. E., *J. Am. Chem. Soc.*, 1985, 107, 5657.
5. Bowyer, W. J.; Merkert, J. W.; Geiger, W. E.; Rheingold, A. L., *Organometallics*, in press.
6. Enlightening discussions are provided in: (a) Geiger, W. E., *Prog. Inorg. Chem.*, 1985, 33, 275; (b) Evans, D. H.; O'Connell, K. M., in "Electroanalytical Chemistry - A Series of Advances", Vol. 14, Bard, A. J., editor, Marcel Dekker, New York, 1986, p. 113.
7. For recent reviews concerned with homogeneous-phase and electrochemical processes, respectively, see: (a) Sutin, N., *Prog. Inorg. Chem.*, 1983, 30, 441; (b) Weaver, M. J., in "Comprehensive Chemical Kinetics", Vol. 27, Compton, R. G., ed., Elsevier, Amsterdam,

1987, Chapter 1.

8. (a) Brunschwig, B. S.; Creutz, C.; McCartney, D. H.; Sham, T.-K.; Sutin, N., *Far. Disc. Chem. Soc.*, 1982, 74, 113; (b) Hupp, J. T.; Weaver, M. J., *J. Phys. Chem.*, 1985, 89, 2795.
9. For energetically symmetrical reactions (i.e. those featuring similar-shaped reactant and product free-energy wells) and in the absence of large driving forces, the preferred (i.e. energetically lowest) transition-state configuration for electron transfer will correspond to an inner-shell configuration essentially midway between the ground-state reactants and products. In the presence of large favorable driving forces, however, the transition-state structure can reflect that of the reactant more closely. In the limit where the free-energy barrier approaches zero, the bond distortional changes will occur entirely after the electron has been transferred.
10. This corresponds to control of the barrier-crossing frequency by nuclear motion rather than by electron tunneling factors associated with donor-acceptor orbital overlap. See ref. 7 for discussions.
11. Nielson, R. M.; McManis, G. E.; Golovin, M. N.; Weaver, M. J., *J. Phys. Chem.*, 1988, 92, 3441.
12. (a) Sumi, H.; Marcus, R. A., *J. Chem. Phys.*, 1986, 84, 4894; (b) Nadler, W.; Marcus, R. A., *J. Chem. Phys.*, 1987, 86, 3906.
13. Jonas, K.; Deffense, E.; Habermann, D., *Angew. Chem. Int. Ed. Engl.*, 1983, 22, 716.
14. Kang, J. W.; Moseley, K.; Maittis, P. M., *J. Am. Chem. Soc.*, 1969, 91, 5970.
15. Rybinskaya, M. I.; Kudinov, A. R.; Kaganovich, V. S., *J. Organomet. Chem.*, 1983, 246, 279.
16. Kölle, U.; Khouzami, F.; Fuss, B., *Angew. Chem. Suppl.*, 1982, 230.
17. Kölle, U.; Fuss, B.; Rajasekharan, M. V.; Ramakrishna, B. L.; Ammeter, J. H.; Böhm, M. C., *J. Am. Chem. Soc.*, 1984, 106, 4152.

18. (a) Perrin, D. D.; Armarego, W. L. F.; Perrin, D. R., "Purification of Laboratory Chemicals", 2nd Edn., Pergamon, New York; (b) Reddick, J. A.; Bunger, Sakano, T. K., "Organic Solvents", Wiley-Interscience, New York, 1986.
19. (a) McManis, G. E.; Golovin, M. N.; Weaver, M. J., J. Phys. Chem., 1986, 90, 6563; (b) Gennett, T.; Milner, D. F.; Weaver, M. J., J. Phys. Chem., 1985, 89, 2787.
20. Nicholson, R. S., Anal. Chem., 1965, 37, 1351.
21. Milner, D. F.; Weaver, M. J., J. Electroanal. Chem., 1987, 222, 21; J. Electroanal. Chem., 1985, 191, 411.
22. Marcus, R. A., J. Phys. Chem., 1963, 67, 853; J. Chem. Phys., 1965, 43, 679.
23. McConnell, H. M., J. Chem. Phys., 1958, 28, 430.
24. For example, see (a) Brown, G. M.; Sutin, N., 1979, 101, 883; (b) Weaver, M. J.; Yee, E. L., Inorg. Chem., 1980, 19, 1936.
25. Hupp, J. T.; Weaver, M. J., J. Electroanal. Chem., 1983, 152, 1.
26. Equation (3) constitutes a more general version of the well-known relation²² $(k_{ox}^o/A_o) = (k_{ox}^h/A_h)^{1/2}$, which follows from Eq. (3) when $r_h = r_o$ so that $C = 0$. However, it is usually expected that $r_o > r_h$ since the reactant is commonly believed to be separated from the electrode by a layer of solvent molecules;²⁷ in this case $C > 0$ so that the use of Eq. (3) is preferred.^{7b}
27. For example, see Weaver, M. J., J. Phys. Chem., 1980, 84, 568.
28. A simplified sample calculation is as follows. By taking the nuclear frequency factor, ν_n , to be $3 \times 10^{12} \text{ s}^{-1}$ (a reasonable value in a "fast" solvent such as acetonitrile or acetone),¹¹ taking the precursor stability constants, K_p , to be 0.6 \AA^{-1} and 0.25 M^{-1} for the electrochemical and homogeneous-phase processes^{19b}, and assuming reaction adiabaticity yields preexponential factors ($A = \nu_n K_p$) of $2 \times 10^4 \text{ cm s}^{-1}$ and $7.5 \times 10^{11} \text{ M}^{-1} \text{ s}^{-1}$, respectively. Inserting, for example, the k_{ox}^o value for $(C_5Me_5)(C_6Me_6)Co^{2+/+}$ in acetone (3.0 cm s^{-1} , Table II) into Eq. (3), and assuming initially that $C = 0$, yields

an estimated k_{ox}^h value of $1.7 \times 10^4 \text{ cm s}^{-1}$. Comparing this with the measured value, $3 \times 10^7 \text{ cm s}^{-1}$ (Table I) suggests that $C \approx 4.5 \text{ kcal mol}^{-1}$. This C value is close to that obtained from Eq. (3a) in acetone with $r_h \approx 7.5 \text{ \AA}$ and $r_o \gg r_h$; the latter inequality is expected if the electrochemical reactant is separated from the electrode by a solvent layer, whereupon $r_o \approx 15\text{-}20 \text{ \AA}$.

29. Merkert, J.; Nielson, R. M.; Weaver, M. J.; Geiger, W. E., J. Am. Chem. Soc., submitted.
30. (a) Nielson, R. M.; McManis, G. E.; Safford, L. K.; Weaver, M. J., J. Phys. Chem., in press; (b) McManis, G. E.; Nielson, R. M.; Gochev, A.; Weaver, M. J., J. Am. Chem. Soc., submitted.
31. Nielson, R. M.; Golovin, M. N.; McManis, G. E.; Weaver, M. J., J. Am. Chem. Soc., 1988, 110, 1745.
32. The proton contact shift of relevance here is between the reduced and oxidized forms of the Rh(III)/(II) and Co(III)/(II) couples, which, for example, in CD_2Cl_2 are 55.0 versus 21.4 ppm for the arene and 121.2 versus 48.5 ppm for the cyclopentadienyl protons.
33. For example, Laviron, E., J. Electroanal. Chem., 1984, 169, 23, 29.
34. For example, Weaver, M. J.; Hupp, J. T., ACS Symp. Ser., 1982, 198, 181.
35. Equation (7) is obtained by noting that the free-energy change for a preceding hapticity step is equivalent to the "precursor" work term w_p discussed in ref. 7b (pp. 3-9), where the activation energy of the overall reaction, ΔG^* , is related to the "intrinsic" barrier in the absence of a driving force, ΔG_{int}^* (i.e. when $w_p = 0$) by $\Delta G^* = \Delta G_{int}^* + 0.5 w_p$ [Eq. (7) of ref. 7b]. [This requires that the transfer coefficient is close to 0.5, as expected for symmetrical (and near-symmetrical) reactions.] Given that here $w_p = -RT \ln K'_{hap}$, we obtain Eq. (7) in the text provided that the preexponential factor for electron transfer remains unaffected by the hapticity step. Similarly, for a hapticity step following electron transfer, the influence upon ΔG^* caused by the "successor" work term w_s can be expressed as $\Delta G^* = \Delta G_{int}^* + 0.5 w_s$ [Eq. (7) of ref. 7]. Since now

$w_s = RT \ln K_{\text{hap}}''$, we recover Eq. (8), again if the electron transfer preexponential factor is unchanged. The negative one-half power in Eq. (8) arises since we define K_{hap}'' as well as K_{hap}' in Eq. (6a) and (5a), respectively, to be the equilibrium constant for the $\eta^6 \rightarrow \eta^4$ transformation.

36. Nielson, R. M.; Weaver, M. J., *J. Electroanal. Chem.*, in press.
37. Borchardt, D.; Wherland, S., *Inorg. Chem.*, 1984, 23, 2537.
38. Gennett, T.; Geiger, W. E.; Willett, B.; Anson, F. C., *J. Electroanal. Chem.*, 1987, 222, 151.

TABLE I. Rate constants for homogeneous-phase self exchange, k_{ex}^{h} ($\text{M}^{-1} \text{s}^{-1}$), of $(\text{C}_5\text{Me}_5)(\text{C}_6\text{Me}_6)\text{M}^{2+/+0}$ redox couples ($\text{M} = \text{Rh}, \text{Co}$) in various solvents at 25°C

Redox Couple	Solvent ^a	C_{D}^{b} mM	C_{P}^{c} mM	k_{ex}^{h} ^d $\text{M}^{-1} \text{s}^{-1}$	$k_{\text{ex}}^{\text{h}}(\text{cor})$ ^e $\text{M}^{-1} \text{s}^{-1}$
Rh(III)/(II)	Acetonitrile	23	1.5	4×10^5	2.5×10^6
Rh(III)/(II)	Acetone	19.5	0.5	3.3×10^5	5×10^6
Rh(II)/(I)	Acetone	7	40.5	8.3×10^2	8.3×10^2
Co(III)/(II)	Acetonitrile	33.5	14	3.0×10^6	2×10^7
Co(III)/(II)	Acetone	30.5	13	1.9×10^6	3×10^7
Co(III)/(II)	Benzonitrile	10	23	3.2×10^6	3×10^7

^a Deuterated solvents were used, except for benzonitrile.

^b Concentration of diamagnetic species [Rh(III), Rh(I), or Co(III)].

^c Concentration of paramagnetic species [Rh(II) or Co(II)].

^d Self-exchange rate constants at 25°C , measured by proton NMR line broadening (see text and ref. 11), for reactant concentrations as indicated alongside. Solutions also contained 0.1 M KPF_6 (for Rh systems) or 0.1 M TEAB (for Co systems) as background electrolyte. Value for Rh(III)/(II) in acetonitrile extrapolated from k_{ex}^{h} values at lower temperatures. See Supplementary Material for detailed NMR parameters.

^e Self-exchange rate constant, corrected for electrostatic work by using Eq. (2) and assuming that $r = 7.6 \text{ \AA}$ (see text). [Note that no correction was necessary for Rh(II)/(I) since the Rh(I) complex is uncharged.]

TABLE II. Rate constants for electrochemical exchange, k_{ox}° , and related parameters for $(C_5Me_5)(C_6Me_6)M^{2+/+/0}$ redox couples ($M = Rh, Co$) at gold in various solvents at 23°C

Solvent	M(III)/(II)			M(II)/(I)		
	$E_{1/2}^a$ V vs. SCE	D^b $10^{-5} \text{ cm}^2 \text{ s}^{-1}$	$k_{ox}^{\circ c}$ cm s^{-1}	$E_{1/2}^a$ V vs. SCE	D^b $10^{-5} \text{ cm}^2 \text{ s}^{-1}$	$k_{ox}^{\circ c}$ cm s^{-1}
$(C_5Me_5)(C_6Me_6)Rh^{2+/+/0}$						
Acetonitrile	-0.62	1.9	0.50	-0.855	2.1	0.018
Acetone	-0.575	2.2	0.31	-0.77	2.5	0.012
Benzonitrile	-0.53	0.29	0.11	-0.85	0.35	5.0×10^{-3}
Nitrobenzene	-0.555	0.25	0.065	<i>d</i>	<i>d</i>	<i>d</i>
Propylene Carbonate	-0.68	0.19	0.090	-0.89	0.22	8×10^{-3}
$(C_5Me_5)(C_6Me_6)Co^{2+/+/0}$						
Acetonitrile	-0.08	1.9	3.0	-1.105	2.1	≈ 5
Acetone	0.05	2.2	0.92	-0.99	2.4	1.5
Benzonitrile	-0.055	0.25	0.085	-1.145	0.34	0.37
Nitrobenzene	0.01	0.15	0.04	<i>d</i>	<i>d</i>	<i>d</i>
Propylene Carbonate	-0.125	0.18	0.06	-1.105	0.27	0.13

^a D.c. polarographic half-wave potential, approximately equal to formal potential of redox couple in listed solvent (see text).

^b Diffusion coefficient of oxidized form of redox couple, obtained from d.c. polarography.

^c Rate constant for electrochemical exchange, obtained in listed solvent containing 0.1 M tetraethylammonium hexafluorophosphate (TBAH). Values obtained by using phase-selective ac voltammetry, except for Rh(II)/(I) which were obtained from cyclic voltammetry (see text).

^d Values could not be obtained due to solvent electroreduction.

TABLE III. Ratios of electrochemical-exchange rate constants in given solvent to that in acetonitrile, $k_{ox}^{\circ}/k_{ox}^{\circ}(AN)$, for mixed-sandwich and related redox couples

Redox Couple ^a	$k_{ox}^{\circ}/k_{ox}^{\circ}(AN)$ ^b			
	Benzonitrile	Nitrobenzene	Propylene Carbonate	Acetone
$(C_5Me_5)(C_6Me_6)Co^{2+/+}$	0.03	0.015	0.02	0.3
$(C_5Me_5)(C_6Me_6)Co^{+/0}$	≈ 0.07		≈ 0.025	≈ 0.3
$(C_5Me_5)(C_6Me_6)Rh^{2+/+}$	0.2	0.13	0.2	0.6
$(C_5Me_5)(C_6Me_6)Rh^{+/0}$	0.3		0.45	0.65
$Cp_2Co^{+/0}$	≤ 0.1 ^c		≤ 0.2 ^c	
$Co(dmgs)_3(BF)_2^{+/0}$	0.35 ^d	0.3 ^d	0.1 ^d	0.65 ^d
$Co(dmgs)_3(BC_4H_9)_2^{+/0}$	0.5 ^d	0.4 ^d	0.4 ^d	1.2 ^d

^a Cp = cyclopentadienyl, dmg = double deprotonated dimethylglyoxime.

^b Ratio of rate constant for electrochemical exchange in indicated solvent to that in acetonitrile, obtained from rate data in Table II unless indicated otherwise.

^c Obtained at mercury electrode in 0.1 M TBAH, from ref. 19a.

^d Obtained at gold electrode in 0.1 M TBAH, from ref. 36.

